We N101 08

Simultaneous Shooting for Sparse OBN 4D Surveys and Deblending Using Modified Radon Operators

R.R. Haacke* (CGG), G. Hampson (Chevron) & B. Golebiowski (CGG)

SUMMARY

Significant gains in productivity (and savings on survey time and cost) have recently been achieved using simultaneous sources with high-density Ocean Bottom Cable geometries. However, where the acquisition is receiver-bound, using sparse Ocean Bottom Node (OBN) arrays for example, the argument for use of simultaneous sources is less compelling. Time and motion analysis for a rolling array of sparse OBN, spaced by 390 m with a 30x30 m shot carpet, shows that time savings of the order of 10 % of the equivalent single-source survey duration should be expected. Although small this may be significant in tightly constrained acquisition seasons. Since time-lapse surveying is the main motivation for many sparse OBN acquisitions, the saving in survey time must be balanced against the risk of additional 4D noise created by simultaneous-source crosstalk. Attenuating crosstalk using a new form of Radon operator implemented with cascaded fx prediction and interpolation as part of a kill-fill process, the level of 4D noise created by simultaneous sources is reduced to an ambient level of 6 %, with a highly randomized character, after imaging.

Introduction

Significant productivity gains have been achieved using simultaneous-source techniques in high-density ocean-bottom cable acquisitions (Walker et al., 2014). In these geometries the survey time is dominated by the source effort. However, it is less clear what impact simultaneous sources may have in sparse Ocean-Bottom Node (OBN) surveys. Such surveys have a high acquisition effort on the receiver side related to the use of submersible remotely-operated vehicles. Since time-lapse monitoring is a strong motivation for sparse OBN acquisition, the impact of simultaneous sources must be assessed in terms of 4D noise and its effect on the interpretation of 4D signals after imaging.

Using survey specifications appropriate for the Gorgon field offshore Western Australia (variable water depths in the range 100-700 m, a square grid of OBN at 390×390 m spacing, and a 30×30 m shot carpet), time and motion studies using a rolling receiver array with two independent source vessels show a saving of approximately 10 % of the survey time compared with single-vessel non-simultaneous acquisition. Although small, this time saving might be significant when the acquisition season is tightly constrained. However, the 10 % saving in time comes with the cost of a second vessel, and also the risk of degrading the final image.

In the following, the impact of simultaneous-source acquisition on a time-lapse OBN campaign is quantified in terms of the change in 4D noise levels compared with equivalent non-simultaneous source data. The impact is assessed using detailed synthetic data with perfectly repeated shot and receiver positions. Crosstalk between the simultaneous sources is attenuated using a new type of Radon-based transform in which the operator copes well with strong, randomised crosstalk. This is used in a *kill-fill* procedure with cascaded fx prediction and interpolation (Guo & Lin, 2003) to achieve an ambient noise level of 6 % after imaging.

Method

The acquisition strategy is depicted in Figure 1a, in which a square OBN array is shot into by two independently operating source vessels. The vessels are separated by an in-line distance of 2 km, with shot-time randomisation (see DeKok & Gillespie, 2002) achieved by vessel independence. This is modelled by randomising a 30 ± 5 minute line-change time and a 6 ± 2 second shot-time interval on the line. Crosstalk randomisation in the common-receiver domain (Hampson et al., 2008) shows the expected dithered character on the in-line section (Figure 1b & 1c), with vessel-2 arrivals distributed randomly within a 4 second window shifted relative to vessel-1 arrivals by the difference in vessel start time on the line. Meanwhile, the crosstalk has a banded-random character on the cross-line section, where the line-change times create random variations in relative start time on the line.

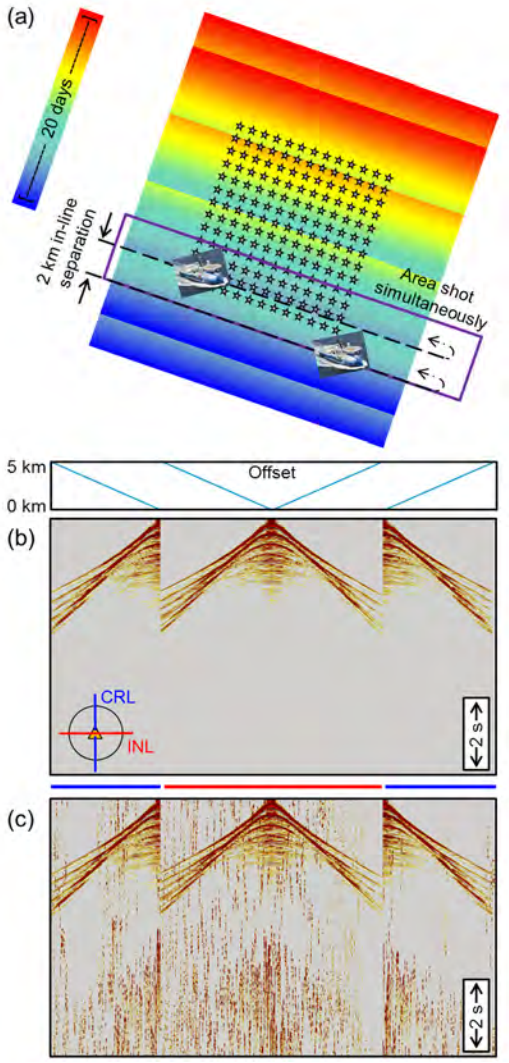

Figure 1 *(a) Simultaneous shooting method using two independent vessels shooting in swaths. (b) Single-source common-receiver gather sectioned by the in-line (red) and the cross-line (blue) intersecting at the receiver. (c) Equivalent simultaneous-source data.*

Crosstalk noise is attenuated using a *kill-fill* procedure (Wang et al., 1989), Figure 2, which reduces incoherent energy in a spatially sorted domain. The *kill* stage seeks to identify and erase regions of data contaminated with the strongest crosstalk. The *fill* stage will interpolate coherent signal into the newly-created gap. Both stages require estimation of coherent signal in the presence of strong, random noise. The creation of a signal model and its difference with the data (the noise model) is illustrated in Figure 3 using input data (Figure 3a) extracted in a 600×600 m block from a common-receiver gather. In the first instance (Figure 3b), an anti-leakage tau-px-py transform is used to create signal and noise models using standard irregular linear Radon operators.

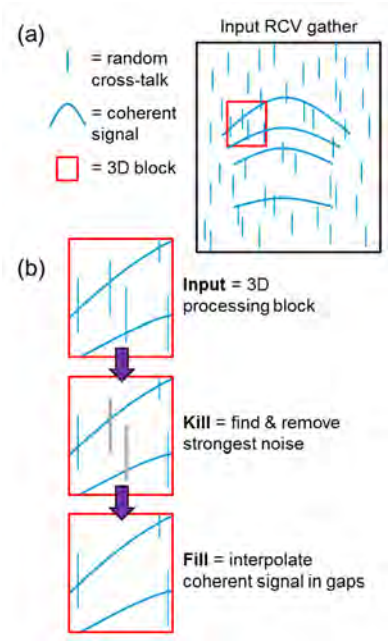

Figure 2 *(a) Signal and crosstalk in a 3D receiver gather. (b) Crosstalk attenuation by the kill-fill process.*

The anti-leakage process (Ng & Perz, 2004) is a sequence of transforms from data space to model space and back, using forward and reverse linear Radon operators to iteratively remove particular slownesses from the input data one-by-one. In this way the effect of one slowness on another (the leakage) is minimised as progress is made through the required range of slownesses. This is represented for a sequence of $k = 1, \dots, M$ slownesses (p_x, p_y) and input data $\boldsymbol{d}(x, y, \omega)$ (with length N, angular frequency $\omega \geq 0$ and $\boldsymbol{d'}_0 = \boldsymbol{d}$) by the recursion,

$$\boldsymbol{d'}_k(x, y, \omega) = \boldsymbol{d}\,'_{k-1}(x, y, \omega) - \boldsymbol{L}^r\left(p_{x_k}, p_{y_k}, \omega\right)\delta_{uv}\boldsymbol{L}^f\left(p_{x_k}, p_{y_k}, \omega\right)\boldsymbol{d'}_{k-1}(x, y, \omega)\,. \tag{1}$$

The k^{th} slowness occurs on row v of $\boldsymbol{L}^f$ and rows $u \neq v$ are eliminated with the Kronecker delta, δ_{uv}. The signal model is given by $\boldsymbol{d} - \boldsymbol{d'}_k$ after k slownesses. In the standard case, operator $\boldsymbol{L}^f$ represents the irregular slant-stack $\boldsymbol{\psi} = \boldsymbol{L}^f\boldsymbol{d}$, over geographic positions x, y, according to

$$\begin{pmatrix} \psi(p_{x_1}, p_{y_1}, \omega) \\ \vdots \\ \psi(p_{x_M}, p_{y_M}, \omega) \end{pmatrix} = \begin{pmatrix} \frac{g_1}{\tilde{g}}e^{i\omega(p_{x_1}x_1 + p_{y_1}y_1)} & \dots & \frac{g_N}{\tilde{g}}e^{i\omega(p_{x_1}x_N + p_{y_1}y_N)} \\ \vdots & \ddots & \vdots \\ \frac{g_1}{\tilde{g}}e^{i\omega(p_{x_M}x_1 + p_{y_M}y_1)} & \dots & \frac{g_N}{\tilde{g}}e^{i\omega(p_{x_M}x_N + p_{y_M}y_N)} \end{pmatrix}\begin{pmatrix} d(x_1, y_1, \omega) \\ \vdots \\ d(x_N, y_N, \omega) \end{pmatrix}, \tag{2}$$

where g is a series of data weights (normalised by their sum, $\tilde{g}$) accounting for the irregular geometry and allowing $\boldsymbol{L}^f$ to evaluate an accurate slowness coefficient $\boldsymbol{\psi}$. Similarly, $\boldsymbol{d} = \boldsymbol{L}^r\boldsymbol{\psi}$, where

$$\boldsymbol{L}^r = \begin{pmatrix} e^{-i\omega(p_{x_1}x_1 + p_{y_1}y_1)} & \dots & e^{-i\omega(p_{x_M}x_1 + p_{y_M}y_1)} \\ \vdots & \ddots & \vdots \\ e^{-i\omega(p_{x_1}x_N + p_{y_1}y_N)} & \dots & e^{-i\omega(p_{x_M}x_N + p_{y_M}y_N)} \end{pmatrix}.$$

The signal estimate incorporates strong crosstalk after relatively few slownesses are processed. This cannot be improved by reducing the number of slownesses processed (increasing the sparseness of the model) without also damaging the signal estimate. The problem is the presence of strong crosstalk affecting the evaluation of the slowness coefficient on the slant-stack in (2), in which the weight of each datapoint on the slant is varied only by the geometric term g. This issue is equivalent to evaluating an expected value from a set of measurements on a slant through the data in which the data errors are not consistent with the probability density function being used to formulate the expectation operator. Better separation of coherent signal from the crosstalk can be achieved by incorporating an expectation operator more accurately representing the data errors (the crosstalk noise). This reduces the effect of strong outliers on the evaluation of the slowness coefficients and produces a more accurate representation of coherent signal in the slowness domain. Then $\boldsymbol{L}^f$ takes the form

$$\boldsymbol{L}^f = \begin{pmatrix} \frac{h_{11}}{\tilde{h}_1}\frac{g_1}{\tilde{g}} e^{i\omega(p_{x_1}x_1+p_{y_1}y_1)} & \cdots & \frac{h_{1N}}{\tilde{h}_1}\frac{g_N}{\tilde{g}} e^{i\omega(p_{x_1}x_N+p_{y_1}y_N)} \\ \vdots & \ddots & \vdots \\ \frac{h_{M1}}{\tilde{h}_M}\frac{g_1}{\tilde{g}} e^{i\omega(p_{x_M}x_1+p_{y_M}y_1)} & \cdots & \frac{h_{MN}}{\tilde{h}_M}\frac{g_N}{\tilde{g}} e^{i\omega(p_{x_M}x_N+p_{y_M}y_N)} \end{pmatrix}, \quad (3)$$

where the new weight h_{nm}, for $n = 1, \dots, N$ and $m = 1, \dots, M$, is an independent probability mass function (normalised by its row-sum, $\tilde{h}_m$) that better represents the data errors. An example for h could be the Laplacian function $h(q) \propto \exp(-|q - \langle q \rangle|/\sigma_q)$ for median $\langle q \rangle$ and variance σ_q. A harsher function could remove outliers completely using a threshold β with $h(q) = 0$ if $\exp(-|q - \langle q \rangle|/\sigma_q) < \beta$ and $h(q) = 1$ otherwise. This selection strategy moves strong crosstalk from the signal model into the noise model and reduces signal leakage in the noise model (Figure 3c).

A further improvement comes by incorporating another layer of data weights into (3). The signal and noise estimates at iteration *k*-1 of the anti-leakage process provide a-priori information on the noise in the data that can be used at iteration *k*. Denoting the envelope function by $\{x\}$ for time-domain data x, the noise-to-signal ratio at iteration *k*-1 is represented by the changemap $C_{k-1} = \{\boldsymbol{d}'_{k-1}/\{\boldsymbol{d} - \boldsymbol{d}'_{k-1}\}\}$. The noisier regions of data are thus down-weighted by updating $h_k = h_{k-1}h_{C_{k-1}}$ where $h_{C_{k-1}}$ is based on the changemap. These self-adapting data weights move more crosstalk into the noise model and further reduce signal leakage (Figure 3d).

The anti-leakage process is typically run conservatively, processing high percentages of slownesses in the data, to attenuate only the strongest crosstalk noise. Lower-amplitude residual noise is subsequently attenuated using cascaded application of fx prediction and interpolation (Guo & Lin, 2003) with increasing sensitivity.

Results

The effect of simultaneous-source acquisition on an OBN time-lapse campaign is quantified in Figure 4. The non-simultaneous source baseline 3D image and baseline – monitor 4D difference (Figure 4a) shows the ideal result with areas of strong 4D signal and areas of weak 4D signal that will test the interpretation from noisier images. The same images produced with simultaneous sources for both baseline and monitor, but using no explicit crosstalk attenuation, are effectively unusable for time-lapse interpretation (Figure 4b). The additional NRMS levels are approximately 70 %. Using the modified-Radon *kill-fill* procedure to attenuate the strongest crosstalk, then applying cascaded fx prediction and interpolation, it is possible to reduce the background NRMS levels to approximately 6 % (Figure 4c). In this case, the weak 4D signal is visible due to its coherence compared with the highly random residual crosstalk noise in the images.

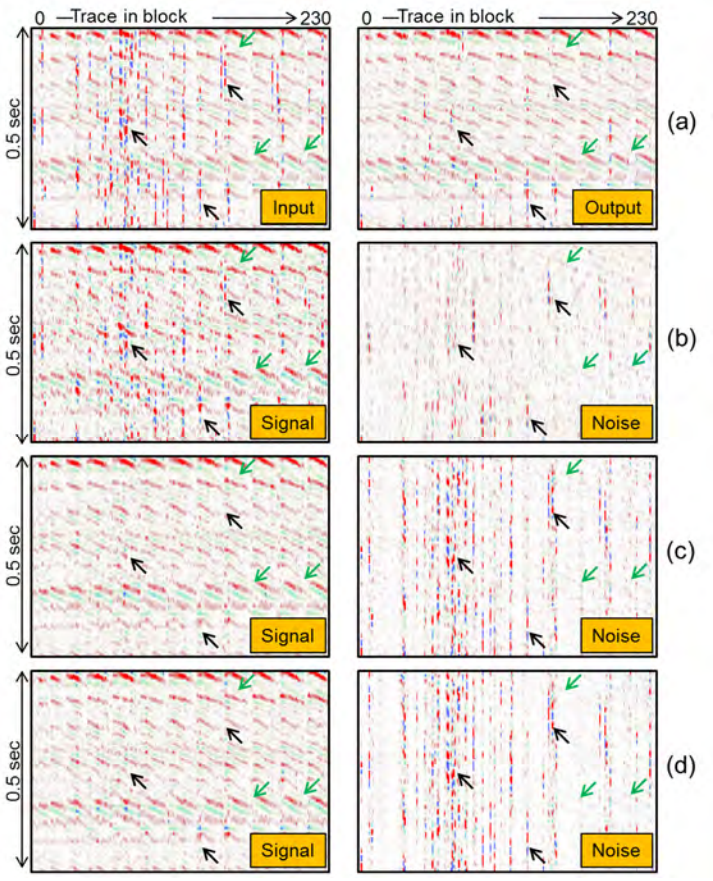

Figure 3 *(a) Input and output 3D processing block. (b) Signal and noise estimates from eq. (2) after 60 % of dips. (c) With the selection strategy. (d) With selection and self-adapting data weights. Crosstalk (black arrows) and signal leakage (green arrows) both improve from (b) to (d).*

Conclusions

Although large productivity gains are possible using simultaneous-sources with high-density ocean-bottom cable geometries, the case for simultaneous-source acquisition is not as strong in surveys using sparse OBN deployed by submersible vehicles. In this study the time saving using two source vessels shooting simultaneously is about 10 % of the equivalent single-vessel survey time without simultaneous shooting. Although small, this may be significant where acquisition seasons are tightly constrained. Using modified Radon operators in an anti-leakage tau-px-py transform followed by residual denoise using fx prediction and interpolation, simultaneous-source crosstalk can be attenuated using *kill-fill* methods to an ambient level of approximately 6 % NRMS in a time-lapse 4D difference.

Acknowledgements

The authors thank CGG and Chevron for data and permission to publish and Chevron for data.

References

DeKok, R., and Gillespie, D. [2002] A universal simultaneous shooting technique. *EAGE 64th Conference & Exhibition*, Extended Abstracts.

Guo, J. and Lin, D. [2003] High-amplitude noise attenuation. *SEG Annual Meeting*, Expanded Abstracts, 1893-1896.

Hampson, G., Stefani, J. and Herkenhoff, F. [2008] Acquisition using simultaneous sources. *The Leading Edge*, **27**, 918-923.

Ng, M. and Perz, M. [2004] High resolution Radon transform in the tx domain using intelligent prioritization of the Gauss-Seidel estimation sequence. *SEG Annual International Meeting*, Expanded Abstracts, 2160-2163.

Walker, C. D. T., Monk, D. J. and Hays, D. B. [2014] Blended source, the future of ocean-bottom seismic acquisition. *EAGE 76th Conference & Exhibition*, Extended Abstracts.

Wang., H., Guangxin, L., Hinz, C. E. and Snyder, F. F. C. [1989] Attenuation of marine coherent noise. *SEG Annual International Meeting*, Expanded Abstracts, 1112-1114.

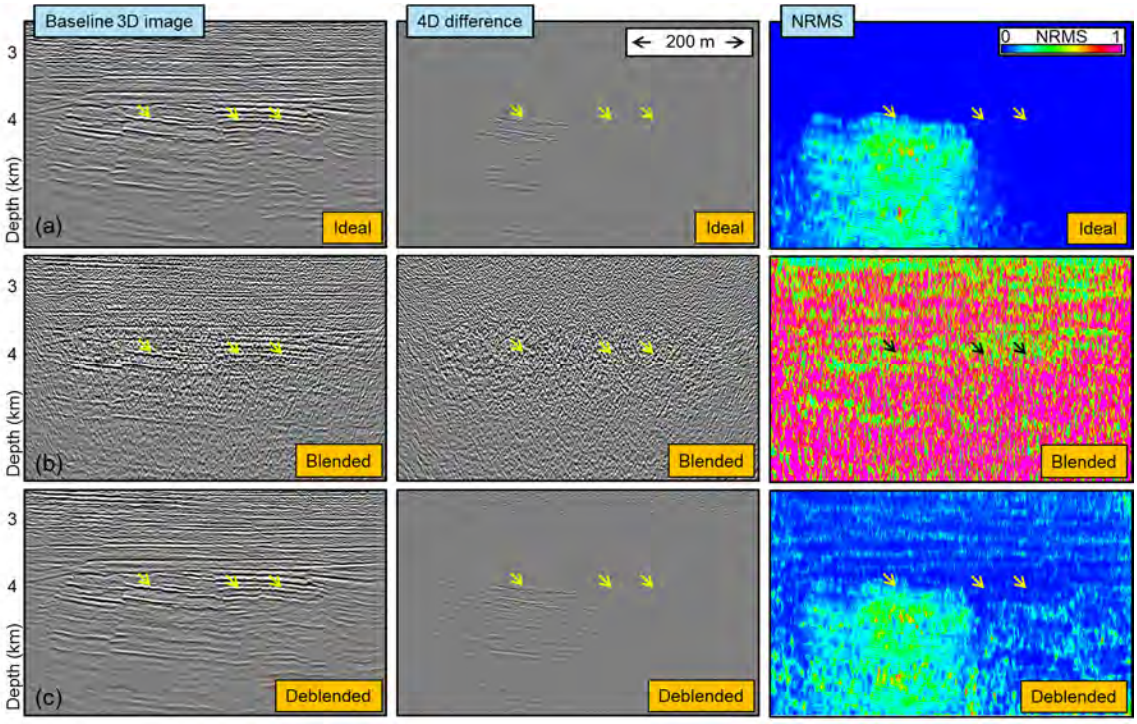

Figure 4 *(a) Single-source Baseline 3D image (left), Monitor – Baseline 4D difference (middle), and NRMS (right). (b) Using simultaneous sources. (c) Using simultaneous sources with kill-fill crosstalk attenuation.*